

RESEARCH ARTICLE | OCTOBER 11 2023

Understanding ac losses in CORC cables of YBCO superconducting tapes by numerical simulations

Linh N. Nguyen   ; Nathaniel Shields  ; Stephen Ashworth; Doan N. Nguyen 

 Check for updates

J. Appl. Phys. 134, 143903 (2023)

<https://doi.org/10.1063/5.0162439>


View
Online


Export
Citation

CrossMark

starting at
EUR 6.360,-



Grows with your experiment.
The MFLI Lock-in Amplifier.

Field-upgradeable options

- 5 MHz frequency extension
- Multi-frequency analysis
- PID controller
- Impedance analyzer

 Zurich Instruments [Find out more](#)

Understanding ac losses in CORC cables of YBCO superconducting tapes by numerical simulations

Cite as: J. Appl. Phys. **134**, 143903 (2023); doi: [10.1063/5.0162439](https://doi.org/10.1063/5.0162439)

Submitted: 14 June 2023 · Accepted: 21 September 2023 ·

Published Online: 11 October 2023



Linh N. Nguyen,^{1,a)} Nathaniel Shields,² Stephen Ashworth,² and Doan N. Nguyen¹

AFFILIATIONS

¹Los Alamos National Laboratory, Los Alamos, New Mexico 87544, USA

²VEIR, Boston, Massachusetts 02210, USA

^{a)}Author to whom correspondence should be addressed: linh@lanl.gov

ABSTRACT

Alternating current (ac) losses in conductor-on-rounded-core (CORC) cables of YBCO high-temperature superconducting (HTS) tapes are a significant challenge in HTS power applications. This study employs two finite element analysis (FEA) models to investigate the contributions from different ac loss components and provide approaches for reducing ac losses in cables. An FEA model based on the T-A formulation treats the cross section of thin superconducting layers as 1D lines and, therefore, only can predict the ac loss generated by the perpendicular magnetic field. In contrast, the model based on H-formulation can be performed on the actual 2D rectangular cross section of HTS tapes to provide the total ac losses generated by magnetic fluxes penetrating from both the edges and surfaces of HTS tapes, although this model requires more computing time and memory. The 1D and 2D simulation models were validated by cross comparing the results from both models and by comparing sub-section and full cross section models. Subsequently, two models relate cable design and operational parameters to the surface and edge losses of a two-layer CORC cable by considering the (1) relative contributions of edge and surface losses to the overall ac losses; (2) effect of the current distribution between inner and outer HTS layers on ac losses; (3) impact of the tape alignment on ac losses in each HTS layer; (4) influence of the thickness of HTS layers on ac losses; (5) effect of size and number of inter-tape gaps on ac losses; and (6) contribution frequency on the ac losses. The research results given in this paper are therefore not only valuable to suggest strategies for reducing ac loss in multi-layer cables but also for developing more accurate and effective methods to calculate ac loss in CORC HTS cables.

Published under an exclusive license by AIP Publishing. <https://doi.org/10.1063/5.0162439>

I. INTRODUCTION

The adoption of conductor-on-rounded-core (CORC) cables of YBCO high-temperature superconducting (HTS) tapes has great potential to enhance the efficiency and capacity of power transmission, yielding more reliable and sustainable electrical grid infrastructure.^{1–5} In CORC cables, superconducting tapes are helically wound around a round core to form a compact, mechanically robust cable structure that can offer high current capacity and excellent flexibility. The helical winding configuration also enables improved current sharing among the tapes, reducing the risk of local hot spots and contributing to a more uniform current distribution. However, ac losses in those HTS cables are still an important technical challenge because they reduce cable efficiency and generate thermal instabilities that may damage the HTS cable. Understanding and reducing ac loss in HTS cables are therefore essential and have been of great research interest, with remarkable

efforts to evaluate and predict ac loss in CORC cables by both experimental^{6–13} and numerical approaches.^{14–34} Ac losses in YBCO tapes are generated by the oscillating movements of flux lines during a cycle. Due to the very high aspect-ratio geometry of YBCO tapes, the magnetic fields applied perpendicular to the wide surface of the tapes (perpendicular magnetic field) generate much higher ac loss than the magnetic fields applied parallel to the wide surface of the tapes (parallel fields). YBCO tapes produced with thin substrates (30 μm) enable the construction of CORC cables with well-conformed tapes, as seen in Fig. 1, which presents the cross section of a CORC cable.^{1,35} CORC reduces the perpendicular magnetic fields applied to the tapes; the field is primarily circumferential. Perpendicular fields only arise in regions near the gaps between tapes (or near the edges of the tapes). We distinguish these losses as the surface loss, generated by flux penetration of the parallel field, and the edge loss, generated by flux penetration of the

30 October 2023 13:53:15

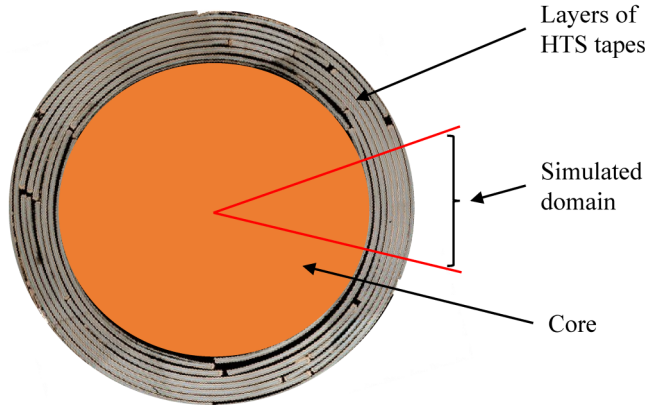


FIG. 1. Cross section of a typical YBCO CORC superconducting cable, consisting of a metal core and HTS tape layers wound around the core. Cable diameter can be varied from one to several centimeters.^{1,35}

perpendicular fields. Similar nomenclature was introduced in Ref. 16 for a CORC cable and¹⁷ for non-inductive coils.

To account for the spiral geometry of the CORC cables when calculating ac losses in CORC cables, 3D FEM COMSOL Multiphysics³⁶ simulations have been used.^{18–21} The 3D models based on the T-A model will underestimate the total ac loss in CORC cables since the surface losses are ignored in these models which treat HTS layers as zero-thickness domains. The 3D models based on H-formulation, however, must artificially increase the modeled thickness of HTS by tens of times to reduce the mesh and computational costs to manageable levels. Such treatment overestimates surface loss and results in a considerable error for scenarios in which surface loss dominates. Ac loss can also be predicted by 2D FEM simulations performed on cable cross sections. Those simulations can be either 1D models, which treat the HTS layers as lines^{22–26} or 2D models based on H-formulation.^{27–32} The 1D models can only calculate edge losses due to ignorance of the thickness of HTS layers. The 2D models, in the meantime, can compute total ac losses which is the sum of the edge and surface losses. Therefore, the use of both 1D and 2D simulations, for the first time, will enable to distinguish the contributions of the edge and surface losses individually.

In this paper, the 1D and 2D simulation models were validated by cross comparing the results from both models and by comparing sub-section and full cross section models. Subsequently, two models were used to study (1) relative contributions of edge and surface losses to the overall ac losses; (2) effect of the current distribution between inner and outer HTS layers on ac losses; (3) impact of the tape alignment on ac losses in each HTS layer; (4) influence of the thickness of HTS layers on surface and edge ac loss components; (5) effect of size and number of inter-tape gaps on ac losses; and (6) contribution frequency on the superconducting and eddy current losses. These results are valuable for minimizing ac loss in multi-layer cables and improving the calculation of ac loss in CORC HTS cables.

TABLE I. Properties of YBCO CORC superconducting cable.

Design	Cable 1	Cable 2
Number of layers	2	2
Number of tapes per layer	8	16
Former diameter (mm)	33.104	33.104
I_c of each HTS tape at 77 K (A)	450	225
Inter-tape gap, gap (mm)	0.5, 1, 1.5, 2	0.5
HTS tape width, w_{HTS} (mm)	12.5, 12, 11.5, 11	5.75
Substrate thickness (μm)	50	50
Copper thickness (μm)	30	30
HTS thickness, t_{HTS} (μm)	1.5–10	1.5

II. CABLE DESIGN AND FINITE ELEMENT SIMULATION MODELS

We focus on two-layer cables. Most of our studies are done on cable 1 in Table I, which consists of 8 tapes per layer. The cable I_c and its former diameter are held constant throughout the studies to generate the same circumferential magnetic field on HTS tapes for all the studies. The width of the tapes is varied about 12 mm as required to adjust the inter-tape gaps. To understand the effect of the number of gaps on cable ac losses, cable 2 (Table I) was used, similar to cable 1, but with double the number of tapes, each with narrower width as detailed in Table I.

A typical YBCO tape includes three electrically conductive constituents: the substrate, the superconducting layer, and the copper/silver stabilizer. All three are considered in our simulations. We only consider ac losses generated in constituent components of the YBCO tapes and ignore the losses generated in the core. Such an approximation is valid if the cable is designed to generate zero axial magnetic fields or the core is made with non-conductive materials. The angle β is defined as the angle between adjacent gaps of the inner and outer HTS layers [see Fig. 2(a)]. With 8 tapes on each layer, β is bounded between 0° to 22.5° . Angle $\beta = 0^\circ$

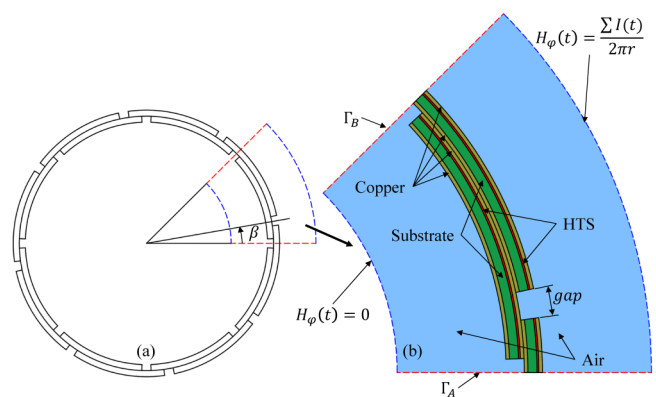


FIG. 2. (a) Cable cross section, illustrating the arrangement of HTS tapes. (b) Enlarged view of the subsector model with periodic boundary conditions imposing on pairs of boundaries, Γ_A and Γ_B .

30 October 2023 13:53:15

TABLE II. Comparing 1D and 2D models in the sub-section and full cross section for a general case with $\beta = 15^\circ$ and for $t = 1.5 \mu\text{m}$, $\text{gap} = 1 \text{ mm}$, $l/l_c = 0.7$.

Models	Types and number of elements			Computational time	Total ac loss (J/m/cycle)	Relative error $(Q_{sub} - Q_{full})/Q_{full} \times 100\%$
	Quad	Edge	Vertex			
$2D_{full}$	50 592	10 960	352	4 h 42 m	$3.2234E \times 10^{-3}$	0.16%
$2D_{sub}$	6324	1494	66	40 m	$3.2287E \times 10^{-3}$	
$1D_{full}$	42 432	9008	288	2 h 31 m	$2.9433E \times 10^{-3}$	0.03%
$1D_{sub}$	5304	1230	54	18 m	$2.9425E \times 10^{-3}$	

From Eqs. (4) and (10)–(12), we find the basic relation

$$\nabla \times \rho \nabla \times \mathbf{H} = -\mu \frac{\partial \mathbf{H}}{\partial t}. \quad (13)$$

Similarly, as in our 1D models, the integration of current density over the cross section of each HTS tape domain should provide the transport current flowing in that tape as seen in Eq. (14). This equation is imposed in weak constraints in our 2D models,

$$I_i = \iint_{\Omega_i} J_z d\Omega_i, \quad (14)$$

where I_i and Ω_i (with $i = \text{inner or outer layer}$) are the transport currents and domains of the inner or outer HTS layers, respectively.

C. Ac loss calculation

Simulations are performed for 1.5 ac cycles and ac losses in each domain are calculated by spatially integrating $\mathbf{J} \cdot \mathbf{E}$ for the last half cycle,

$$Q = 2 \int_{1/f}^{3/(2f)} \int_{\Omega} \mathbf{J} \cdot \mathbf{E} d\Omega dt, \quad (15)$$

where Ω represents the superconducting domain and f denotes the frequency of the applied ac source.

D. Boundary conditions and meshing

In order to include the surface loss in 2D simulations, meshing with several nodes along the thickness on HTS layers is sufficient. In this paper, meshing with four to six nodes along the HTS layer thickness was used in 2D simulations to accurately calculate the total ac loss in HTS tapes with finite thickness. To reduce the computational workload, simulations were performed only in a sub-section of the cross section enclosed by a pair of boundaries, Γ_A and Γ_B as seen in Fig. 2. In special cases of fully aligned or fully misaligned configurations, boundaries Γ_A and Γ_B can be set as perfect magnetic boundary. For a general case with arbitrary arrangement of HTS tapes in the two layers ($0^\circ < \beta < 22.5^\circ$), periodic boundary conditions must be set on those boundaries. Both 1D and 2D models performed on the sub-section with periodic boundary conditions were compared and validated to the similar simulations performed on the entire cross section of the cables. All the simulations were executed on a workstation laptop equipped with an Intel(R) Xeon(R) W-11855M CPU

@ 3.20 Gz and 128 GB RAM. Table II summarizes the computational loads and results obtained from both 1D and 2D models performed in the sub-section and full cross section for the general case with $\beta = 15^\circ$. The computational times for the 2D models performed on the sub-section and full cross section were about 40 min and about 4 h 42 min, respectively. Relative error of the calculated losses between the two 2D models was under 0.2%. Thus, for 2D H-formulation models, simulations on the sub-section with periodic boundary conditions can reduce the computation time by about 80%–90% while reproduce the same results as the standard simulations performed on the full cross sections. This statement is also true for the 1D T-A models as seen in Table II. For 1D T-A models, computational time reduces from 2 h 31 min in a full cross section simulation to about 18 min for the sub-section simulation. The relative errors of the calculated losses between the two 1D simulations are under 0.05%. In conclusion, comparison confirmed that the use of periodic boundary conditions enables both 1D and 2D simulations to be performed in a sub-section to significantly reduce the computational workload without losing the accuracy.

III. RESULTS

Our analysis focuses on the geometric cases in which ac losses are expected to be the highest and the lowest: (1) the fully aligned arrangement ($\beta = 0^\circ$), wherein the enhanced perpendicular magnetic field should generate the highest ac losses and (2) the fully misaligned arrangement ($\beta = 22.5^\circ$), wherein the reduced perpendicular magnetic field should generate the lowest ac losses. When β is varied from ($\beta = 0^\circ$) to ($\beta = 22.5^\circ$), ac losses are expected to vary between the values of the two extreme cases; Sec. III E presents that data. All simulations assume good current distribution (i.e., the inner and outer layers carry the same transport current), but for those in Sec. III C where the impact of current distribution on ac losses is presented. Also, most of the results were calculated at standard frequency $f = 50 \text{ Hz}$, except for the simulations in Sec. III F where the impact of frequency on ac losses is presented. The parameters used are described in Table III.

A. Effect of t_{HTS} on ac losses

Figure 4 provides a comparison of edge loss $Q_{edge} = Q_{1D}$ (calculated using 1D models) and total losses, $Q_{total} = Q_{2D}$ (obtained from 2D models) in cable 1, with t_{HTS} varying from 1.5 to 10 μm . We simulate both the fully aligned and fully misaligned cases. We set a gap of 1 mm. As expected, for the same thickness of HTS layers, the ac losses generated in the fully aligned arrangement are significantly higher (more than double) than those generated in the

TABLE III. Description of parameters.

Parameter	Description
t_{HTS}	Thickness of HTS layers
gap	Size of inter-tape gaps
Q_{edge} or Q_{1D}	Ac loss generated near the edges by perpendicular fields
$Q_{surface}$	Ac loss generated by parallel magnetic fields
Q_{total} or Q_{2D}	Total ac losses calculated from 2D models
I_{inner}	Current in the inner layer
I_{outer}	Current in the outer layer
I	Total current of the cable

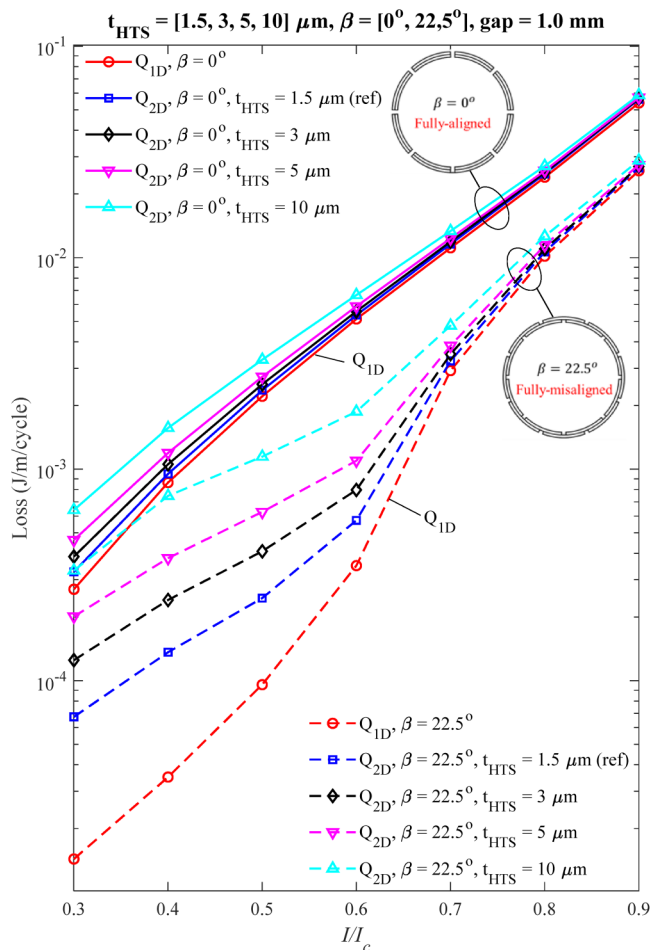


FIG. 4. The edge losses (calculated using the 1D model) and total losses (obtained from the 2D model) in cable 1 with t_{HTS} varying from $1.5 \mu\text{m}$ to $10 \mu\text{m}$. Losses are plotted against the normalized current I/I_c for both cases, $\beta = 0^\circ$ (fully aligned) and $\beta = 22.5^\circ$ (fully misaligned).

misaligned case, indicating that the contribution of the edge losses is more significant in the fully aligned arrangement. The contribution of edge losses is expected to increase with increasing gap and the effect of the gap on ac losses will be further discussed in Sec. III B.

Because the 1D model only captures the edge ac losses, the difference between ac losses calculated by our 2D models and 1D models is the surface loss, $Q_{surface} = Q_{2D} - Q_{1D}$. The contribution of $Q_{surface}$ increases with the thickness of the HTS layers, especially for the case of fully misaligned arrangement, $\beta = 22.5^\circ$. To further analyze the effect of t_{HTS} on the contribution of $Q_{surface}$ and Q_{edge} , ac losses plotted in Fig. 4 are normalized to $Q_{2D} - 1.5 \mu\text{m}$, the total loss calculated for a cable with $t_{HTS} = 1.5 \mu\text{m}$, close to the actual thickness of HTS layers in standard commercial tapes. The normalized losses, $Q/Q_{2D} - 1.5 \mu\text{m}$, are plotted in Figs. 5(a) and 5(b) for the fully aligned case and fully misaligned case, respectively. For the fully aligned case [Fig. 5(a)], the 1D model underestimates the loss by around 20% when I/I_c is equal to 0.3. However, when I/I_c exceeds 0.6, the 1D model only underestimates the loss by 5%. Artificially increasing t_{HTS} results in a considerable overestimation of ac loss. For instance, if t_{HTS} increases from 1.5 to $10 \mu\text{m}$, ac loss increases by nearly 200% at $I/I_c = 0.3$, by $\sim 40\%$ at $I/I_c = 0.5$ and by $\sim 5\%$ at $I/I_c = 0.9$.

For the fully misaligned case [Fig. 5(b)], the effect of t_{HTS} on the cable ac loss is more significant. The 1D model underestimates the loss by around 80% when I/I_c is equal to 0.3. However, when I/I_c exceeds 0.7, the difference in loss estimation reduces to less than 10% [Fig. 5(b)]. Artificial increases of t_{HTS} significantly overestimate ac loss in the cable. For instance, increasing t_{HTS} from 1.5 to $10 \mu\text{m}$ results in an increase in cable ac losses by 500% at $I/I_c = 0.3$, by $\sim 330\%$ at $I/I_c = 0.6$ and by $\sim 10\%$ at $I/I_c = 0.9$.

Our 2D simulations utilize mesh with four elements along the thickness of HTS tapes to accurately calculate ac loss for the cable in any cases. Our computational testing has indicated that 2D simulations using a one-element mesh along t_{HTS} can significantly reduce the computational time and may also decrease overestimation of ac loss due to artificial increasing t_{HTS} .³⁸ However, this approach may introduce some considerable errors by underestimating magnetization loss generated by parallel circumferential fields. Figure 6 compares losses calculated by 2D models using one-element and four-element meshing along t_{HTS} . For the fully aligned case where the edge loss dominates [see Fig. 6(a)], the loss calculated by the 2D model using one element for various t_{HTS} is the same as that obtained from the 1D model. However, when $I/I_c < 0.6$, the loss calculated by the 2D model using one element is slightly lower than loss calculated by the 2D model using four elements for the case with $t_{HTS} = 1.5 \mu\text{m}$ (close to the actual tape thickness). In the case of the fully misaligned configuration, the 2D model using one element significantly underestimates the total ac loss as seen in Fig. 6(b). Again, the losses calculated by the 2D model using one element are very close to those obtained from the 1D model and significantly lower than the total losses calculated by the 2D model using four elements for the cable using a tape with $t_{HTS} = 1.5 \mu\text{m}$ (close to the actual tape thickness). That underestimation is more significant in the lower current region where surface magnetization loss caused by the parallel field is dominant.

30 October 2023 13:53:15

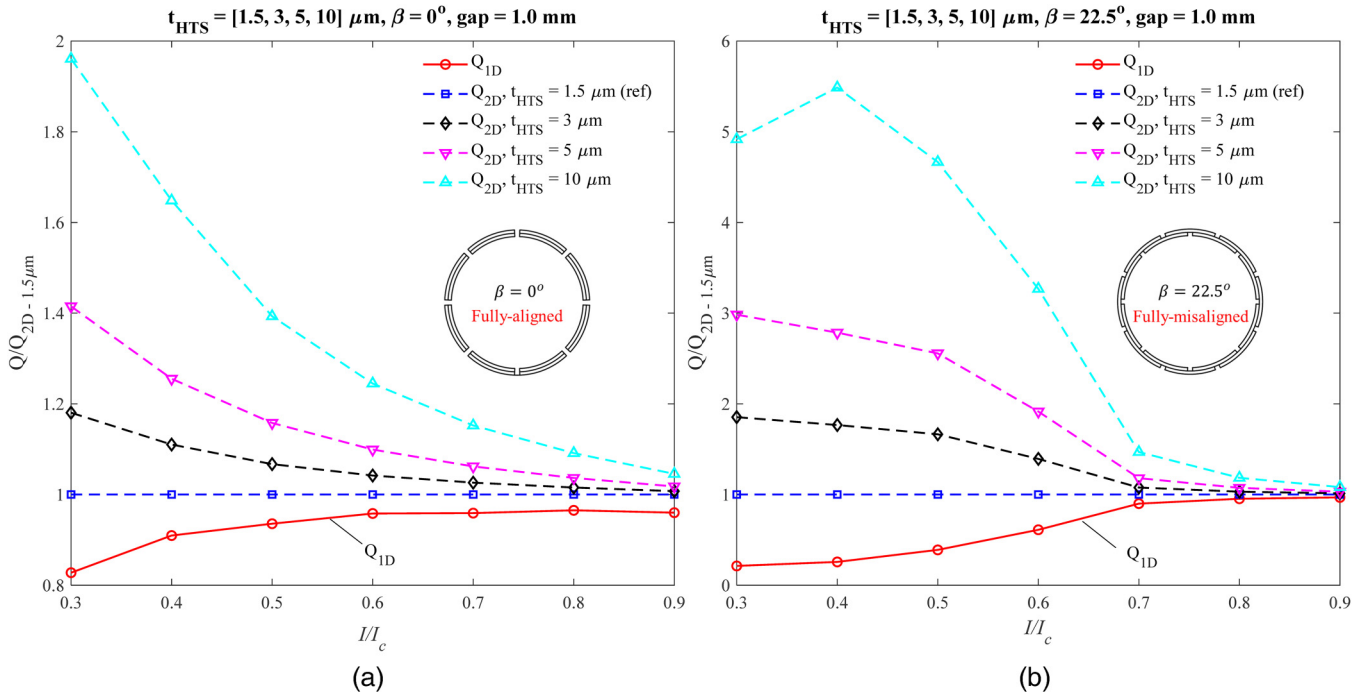


FIG. 5. Normalized ac losses $Q/Q_{2D-1.5\mu m}$, where Q are ac losses plotted in Fig. 4 and $Q_{2D-1.5\mu m}$ is the total loss calculated by the 2D model for a cable of standard YBCO tapes ($t_{HTS} = 1.5 \mu m$). Losses are plotted against the normalized current I/I_c for two cases: (a) $\beta = 0^\circ$ and (b) $\beta = 22.5^\circ$.

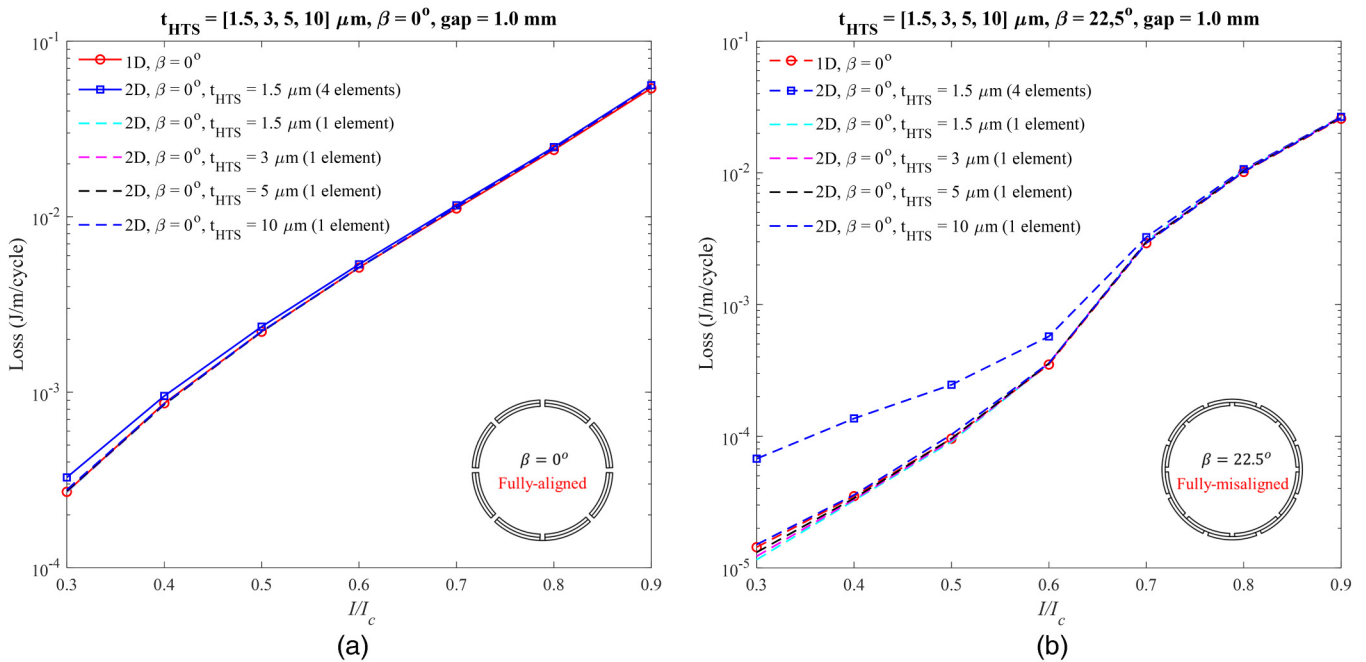


FIG. 6. Comparing ac losses calculated by 2D models using one-element and four-element meshing along t_{HTS} for two cases: (a) $\beta = 0^\circ$ and (b) $\beta = 22.5^\circ$.

30 October 2023 13:53:15

In summary, it appears that the 2D model using only one element yields results that are very similar to the 1D model. Consequently, it fails to account for surface losses, which can be a significant component of ac losses in certain scenarios. On the other hand, the 2D model using multiple elements along the tape's thickness can offer accurate calculations of ac losses in any cases.

B. Effect of the gap on cable ac losses

Figure 7 illustrates the effect of various values of gap ranging from 0.5 to 2 mm on cable ac losses for the case of fully aligned arrangement. Results obtained from both 1D and 2D models, along with $Q_{surface} = Q_{2D} - Q_{1D}$ are all plotted in Fig. 7 to establish the contributions of Q_{edge} and $Q_{surface}$ for various values of gap and transport current. In general, larger gaps lead to higher total losses, as expected. Ac losses increase by about 4 to 7 times as the gap increase from 0.5 mm to 2 mm, depending on the value of the

transport current. The contribution of Q_{edge} is calculated by our 1D model is dominant and increases quickly with increasing transport current. Q_{edge} is roughly proportional to $(I/I_c)^{4.5}$. For gaps larger than 1.5 mm and $I/I_c > 0.5$, edge loss contributes more than 90% of the total loss. The 1D model can be used to predict ac losses with acceptable error for these cases. For gap = 0.5 mm, the contribution of Q_{edge} increases from 50% at $I/I_c = 0.3$ to ~95% at $I/I_c = 0.9$ of the total losses.

The surface loss, $Q_{surface}$, is nearly independent of the size of gap at $I/I_c < 0.6$. $Q_{surface}$ slightly increases for larger gaps at high currents, $I/I_c > 0.6$. $Q_{surface}$ increases with current at a slowly compared to Q_{edge} because $Q_{surface}$ is roughly proportional to $(I/I_c)^2$. Based on the results plotted in the figure, the contribution of $Q_{surface}$ is only larger than ~10% of the total loss when the gap is small (< 0.5 mm) and at low current ($I/I_c < 0.6$). The 2D model is therefore preferable.

Figure 8 depicts the effect of various gap values ranging from 0.5 to 2 mm on cable ac losses for the fully misaligned

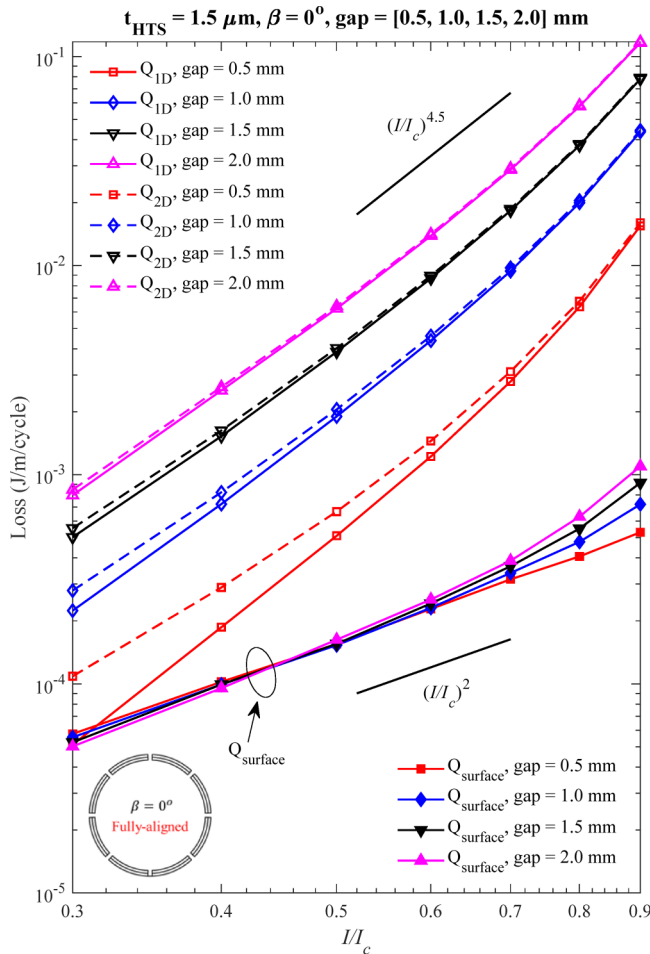


FIG. 7. Ac losses obtained from 1D and 2D models are plotted against the normalized current I/I_c for the case of $\beta = 0^\circ$.

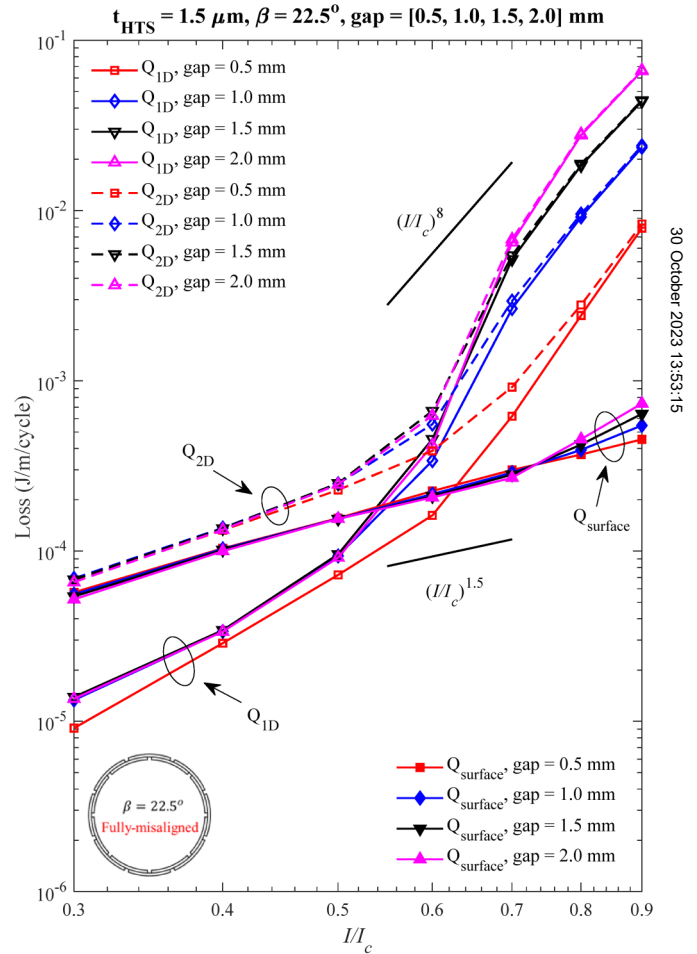


FIG. 8. Ac losses obtained from 1D and 2D models are plotted against the normalized current I/I_c for the case of $\beta = 22.5^\circ$.

30 October 2023 13:53:15

configuration. Results obtained from both 1D and 2D models along with $Q_{surface} = Q_{2D} - Q_{1D}$ are also plotted. Again, $Q_{surface}$ is nearly independent of the gap for quite a wide range of transport currents, $I/I_c < 0.75$. The slopes of both Q_{edge} and $Q_{surface}$ curves change with the transport current. However, in general, Q_{edge} increases with transport current at a much faster rate than $Q_{surface}$.

For low currents, the ac losses calculated by the 2D model are significantly higher than those calculated by the 1D model, indicating that $Q_{surface}$ is dominant. Thus, cable ac losses are independent of the gap when $I/I_c < 0.5$. At higher currents, the contribution from Q_{edge} becomes more significant when the current increases—the 1D results approach the results obtained from the 2D model. Hence, the effect of the gap size on the cable ac losses becomes more significant as current increases. At $I/I_c = 0.9$, the cable total ac losses increase 600% when the gap increases from 0.5 to 2 mm. In conclusion, the effect of gap size on cable ac losses for the fully misaligned case strongly depends on the transport current, which determines the relative contribution of the surface and edge losses.

C. Effect of the current distribution on ac losses

Cables are usually designed to have perfectly balanced current distribution between the layers. However, this condition can be difficult to achieve, and cables may operate with unbalanced current distribution as in Refs. 1 and 8. Establishing the relationship between layer current distribution and loss is therefore useful. Figure 9 illustrates the analysis of ac losses obtained from the 2D model for different transport current distribution ratios, I_{inner}/I . Here, I_{inner} is the current in the inner layer and I is the total

current in the cable. We compute losses for three values of gap, gap = 0.5, 1, and 1.5 mm, and three values of the transport current, $I = 0.5I_c$, $0.7I_c$, and $0.9I_c$. Results for both the fully aligned and fully misaligned cases are depicted in Figs. 9(a) and 9(b), respectively. In general, the lowest ac losses are identified at or near $I_{inner}/I = 0.5$ (well-balanced current sharing) for all the data in both figures. The effect of the off-balanced current sharing on total ac losses is stronger at the higher cable transport currents and smaller gaps, no matter whether the inner layer carries either more or less than the outer layers. It is well known that the transport ac losses increase significantly with increasing transport current, especially when the transport current approaches the critical current of the conductor. Therefore, the unbalance of current sharing at higher cable transport current will push a very high transport electrical current in one layer (either the inner or outer layers). Consequently, that layer will generate significantly higher ac loss, increasing the cable total ac losses. Therefore, the overall impact of the off-balanced current sharing on the total cable ac losses is considerably stronger at higher cable transport current. Similar behaviors have been observed experimentally in Refs. 33 and 34.

D. Individual contribution of ac loss in the inner and outer layers

Despite the inner and outer layers carrying balanced current, they are expected to experience distinct magnetic fields and generate varying ac losses. Figure 10 illustrates the ac loss curves for both tape arrangements, obtained from either the 1D model [Fig. 10(a)] or the 2D model [Fig. 10(b)]. The results from the 1D model

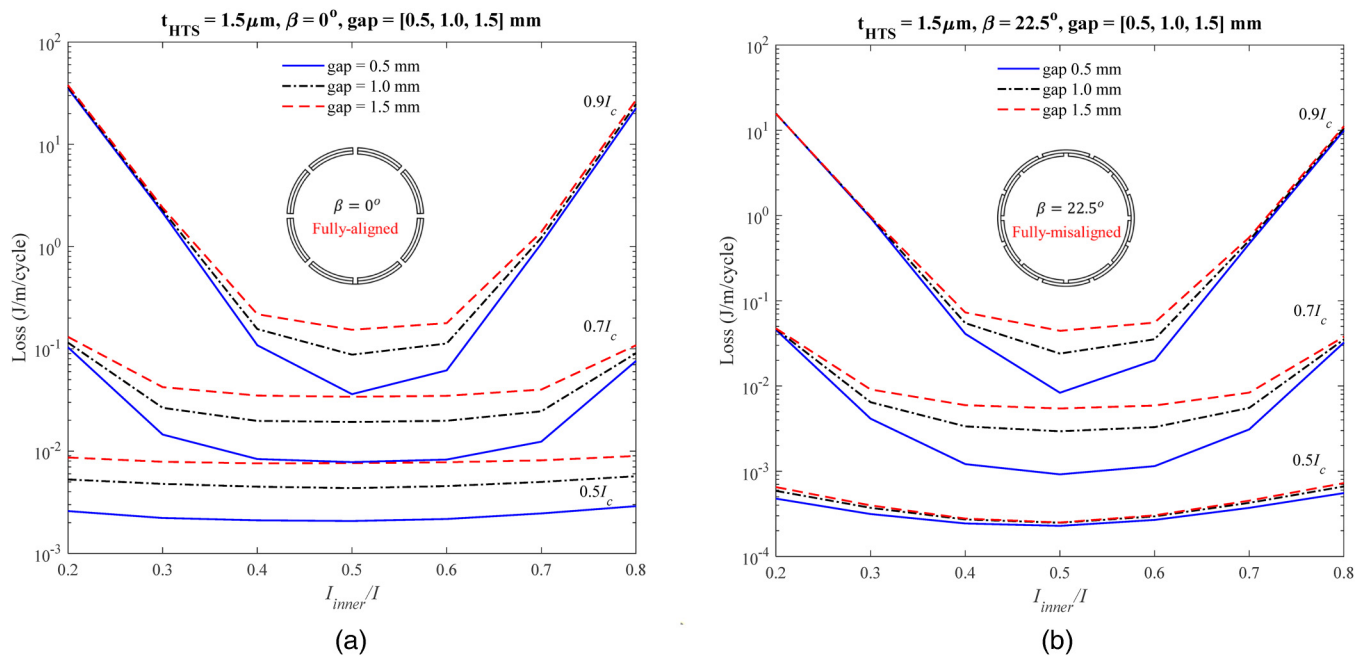


FIG. 9. Ac losses in cable 1 as a function of the transport current distribution ratio I_{inner}/I for both cases, (a) $\beta = 0^\circ$ and (b) $\beta = 22.5^\circ$.

30 October 2023 13:53:15

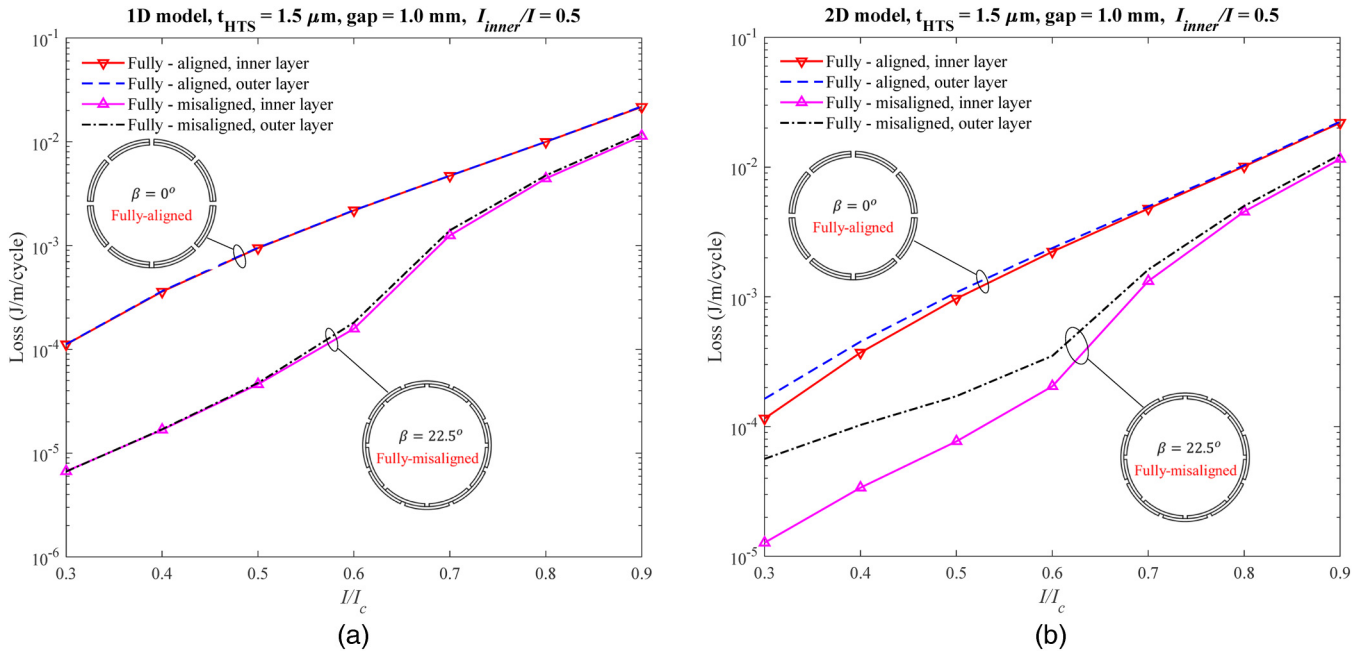


FIG. 10. Ac losses generated in the inner and outer layers as functions of the normalized current I/I_c calculated by (a) 1D model and (b) 2D model.

depicted in Fig. 10(a) show that the inner and outer layers generate nearly same edge loss for either $\beta = 0^\circ$ or $\beta = 22.5^\circ$. Conversely, the results depicted in Fig. 10(b) demonstrate that the outer layer generates slightly higher ac losses in both the fully aligned and fully

misaligned cases. Nonetheless, the discrepancy in ac loss is more notable at lower I/I_c s, due to the dominance of surface loss in the low current region, as discussed in Sec. III B. This outcome is to be expected, as the outer layer experiences higher parallel fields,

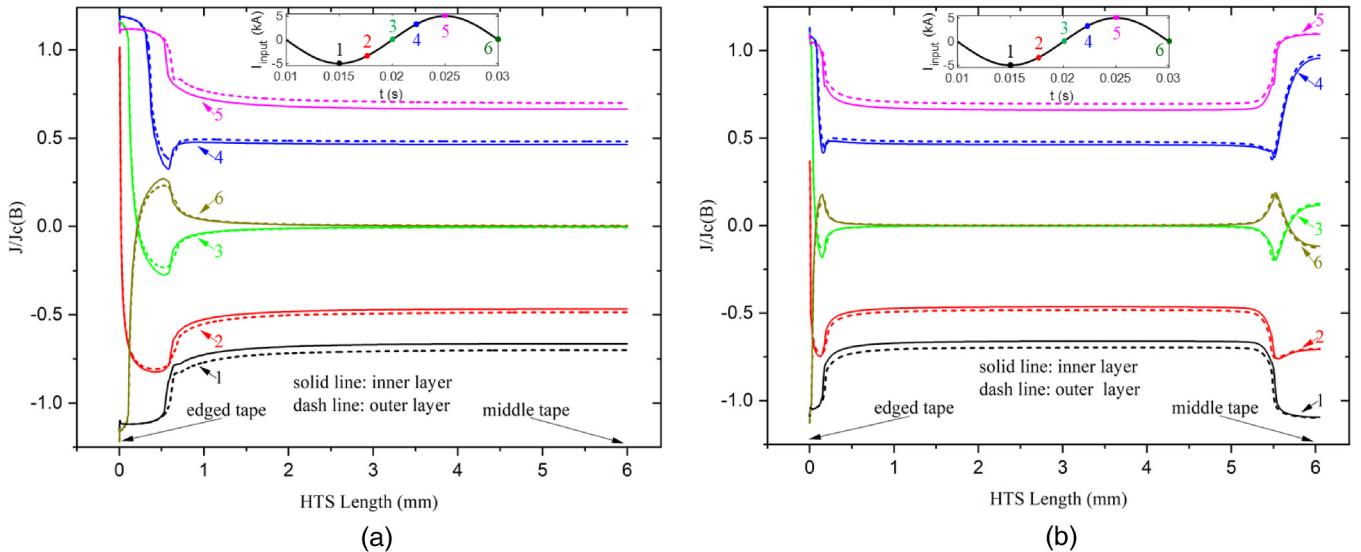


FIG. 11. Distribution of the normalized current density $J/J_c(B)$ along the half-width of HTS tapes in both inner and outer layers at several points during an ac cycle for (a) $\beta = 0^\circ$ and (b) $\beta = 22.5^\circ$.

30 October 2023 13:53:15

yielding higher surface losses. To confirm the results shown in Fig. 10 and visualize the electrodynamics of the HTS tapes, the current profiles along the half-width of HTS tapes in both inner and outer layers at several points during an ac cycle are depicted in Fig. 11. The current profiles are plotted at 6 points labeled 1–6, as seen in the insets of those figures. The evolutions of the current distribution are nearly the same for the inner and outer layers. At each time step, the current density in the outer layer seems to be slightly higher, generating higher ac losses as seen in Fig. 10. The current density reaches or slightly surpasses $J_c(\mathbf{B})$ in small regions near the gaps where they experience the application of the perpendicular magnetic field.

Figure 12 shows the ac loss contribution from the inner and outer layers when the current sharing is unbalanced with the current sharing ratio of $I_{inner} : I_{outer} = 0.4 : 0.6$ and $0.6 : 0.4$ for both fully aligned and fully misaligned cases. As seen in Fig. 10, the inner and outer layers generate nearly same ac losses when they carry the same currents. When the current sharing is unbalanced, the ac losses are generally higher in layer carrying higher transport current

current, as expected. However, there is a small interesting exception for the case of fully misaligned configuration and $I_{inner} : I_{outer} = 0.6 : 0.4$. In this case, the outer layer carries only two-thirds of the current carried in the inner layer, but it generates higher ac loss when $I/I_c < 0.45$. This is explained by the dominant contribution of the surface loss at lower transport current region in the case of the fully misaligned configuration and much higher surface loss generated in the outer layer which is always subjected to higher circumferential magnetic field. When $I/I_c > 0.5$, the transport loss becomes dominated and the inner layer generate higher ac loss since it carries higher transport current.

E. Effect of the HTS tape arrangement on ac losses

To achieve balanced cables, the inner and outer layers are wound in opposite directions. Therefore, angle β varies from 0° to 22.5° as discussed prior. Figure 13 plots the dependence of the total ac losses on β for several values of transport current and gap for $t_{HTS} = 1.5 \mu\text{m}$. Generally, the ac losses are the highest near

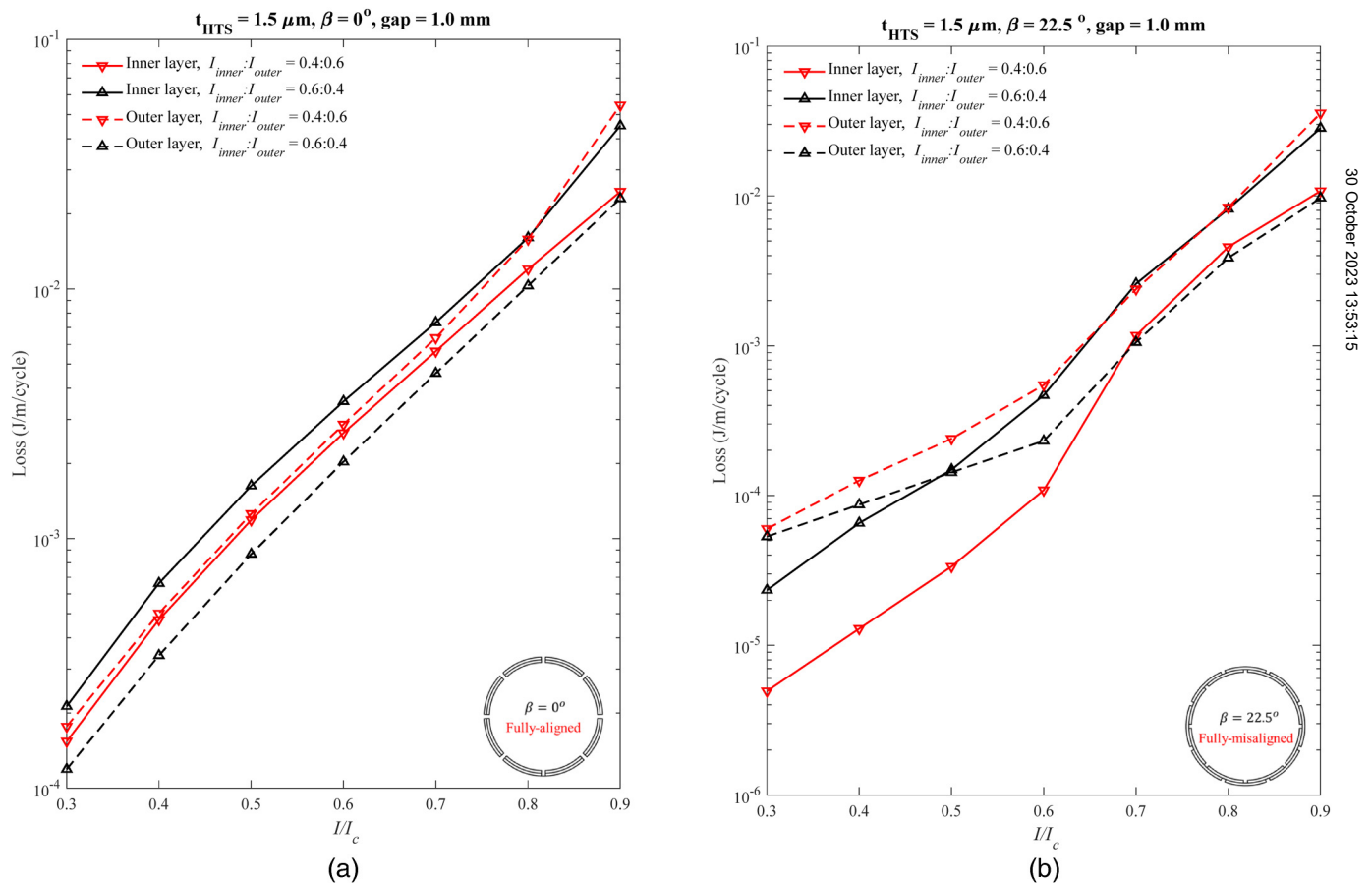


FIG. 12. Ac losses generated in the inner and outer layers as functions of the normalized current I/I_c with $I_{inner} : I_{outer} = 0.4 : 0.6, 0.6 : 0.4$ for (a) the fully aligned case and (b) the fully misaligned case.

30 October 2023 13:53:15

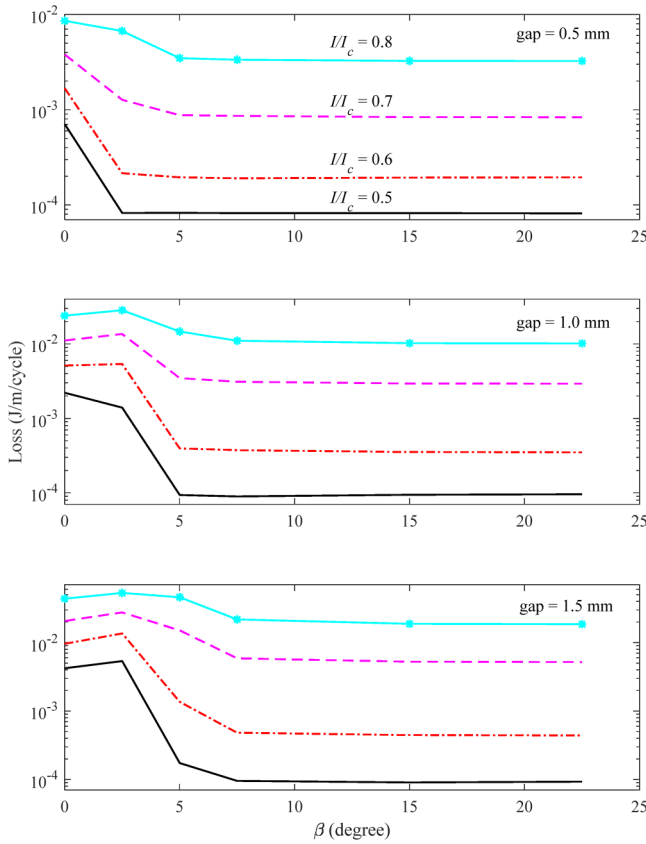


FIG. 13. Total ac loss in cable 1 as functions of β for different gaps (gap = 0.5 mm, 1 mm, and 1.5 mm) and at different values of the transport current ($I = 0.5I_c, 0.6I_c, 0.7I_c$ and $0.8I_c$).

$\beta = 0^\circ$ and the lowest when $\beta = 22.5^\circ$, as expected. For gap = 0.5 mm, ac losses quickly decrease when β increases, and the ac losses are minimal for $\beta > 5^\circ$; perpendicular fields are only present near gaps, and magnetic flux lines quickly align to the tapes' surface away from those gaps. Hence magnetic fields realized on the HTS tapes are nearly identical for β between 5° and 22.5° .

For larger gaps, the effect of β on the total ac losses is similar. However, for those larger gaps, maximal ac losses are observed when β is a few degrees shifted from 0° , suggesting a higher magnetic field in this configuration.

The results in Fig. 13 suggested a possible improvement in predicting the total ac losses in CORC cables. While the calculation of ac losses at $\beta = 0^\circ$ and $\beta = 22.5^\circ$ can basically provide the highest and lowest values, the average ac losses calculated from the curves in Fig. 13 for the entire range of β would provide a better estimation of ac losses in cables.

F. Effect of frequency on ac loss in cables

The ac losses in HTS originates from (1) flux-creep loss, which is hysteretic in nature and dominates at for low transport

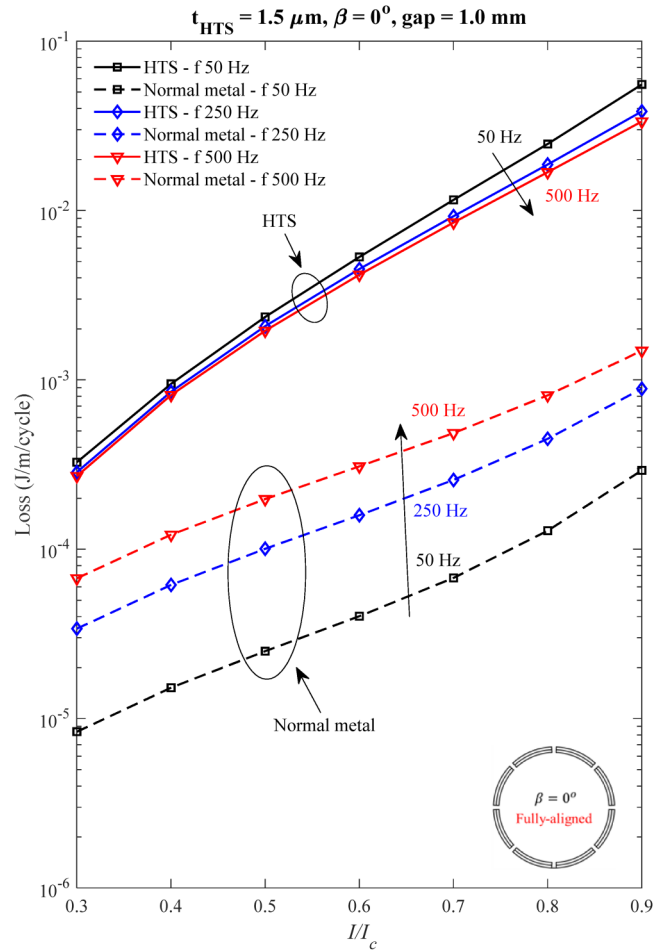


FIG. 14. Ac losses in the HTS layers and normal metal layers at 50, 250, and 500 Hz for the fully aligned case.

currents, and (2) flux-flow loss, which is resistive in nature and dominates for high transport currents. Induced currents generated in normal metal layers (substrates and stabilizers) also generate the eddy current losses. Because these three losses depend differently on frequency, we simulate three frequencies of 50, 250, and 500 Hz.

Figure 14 plots the total ac losses per cycle in the HTS and non-superconducting layers at 50, 250, and 500 Hz for the fully aligned case. Generally, the losses in normal metal layers are significantly lower than those generated in HTS layers. The eddy current loss in normal metal per an ac cycle seems to be proportional to the frequency as expected. The ac losses in the HTS layer slightly decrease with increasing frequency and that decrease becomes more considerable at higher currents. This behavior suggests that there may be a contribution of the flux-flow loss (which is proportional to $1/f$), and that contribution is greater with increasing transport current as expected.

30 October 2023 13:53:15

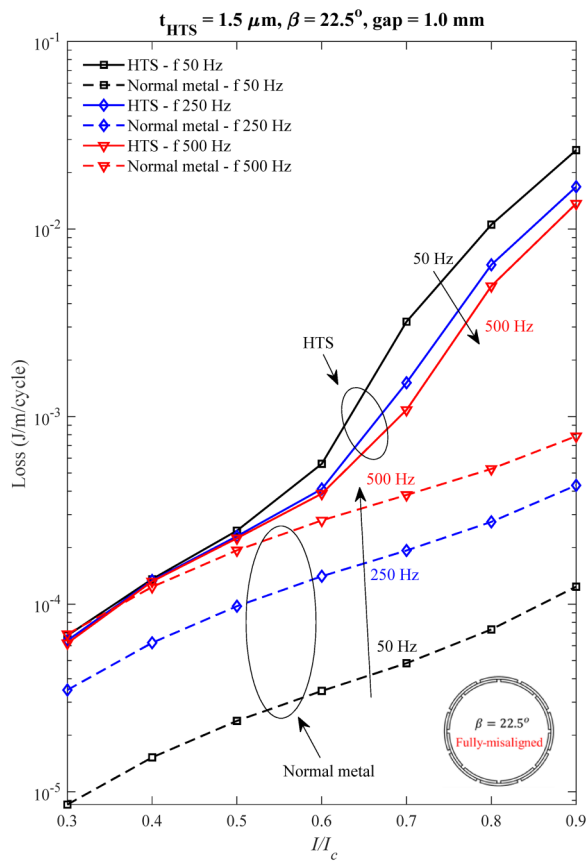


FIG. 15. Ac losses in the HTS layers and normal metal layers at 50, 250, and 500 Hz for the fully misaligned case.

Figure 15 plots ac losses in the HTS and normal metal layers at 50, 250, and 500 Hz for the case of $\beta = 22.5^\circ$. Again, the eddy current loss per cycle of the normal metal layers also increases proportionally to frequency. Though the HTS losses are lower for this case ($\beta = 22.5^\circ$) in comparison to the case of $\beta = 0^\circ$, they are still higher than the eddy current losses when $I/I_c > 0.6$. The HTS losses are independent of frequency for $I/I_c < 0.5$, implying that flux creep loss is dominant. The situation is changed drastically when the transport current increases to higher values. The HTS ac loss decreases with increasing frequency for $I/I_c > 0.7$.

To make explicit the effect of frequency on the ac losses in the HTS, the perpendicular magnetic fields applied along the half-width of HTS tapes are calculated at the positive peak current of $I = 0.7I_c$ and are plotted in Fig. 16 (for the case $\beta = 0^\circ$) and Fig. 17 (for the case $\beta = 22.5^\circ$). The half-width of the HTS tape of the inner layer is denoted as arc-length AB and the half-width of the HTS tape of the outer layer is denoted as arc-length CD (see Figs. 16 and 17). As expected, the perpendicular fields are only non-zero at small regions very close to the gaps. The rest of the tape width experiences no perpendicular fields. In both Figs. 16 and 17, the perpendicular magnetic fields are slightly higher when the frequency is lower, causing higher ac loss at lower frequencies, as seen in Figs. 14 and 15. There is no clear explanation for this observation, but the shielding effect of the HTS layers and metal layers might contribute. Few studies have been done to measure or calculate ac losses in CORC cables at several frequencies to mainly understand the contribution of eddy current losses in the metal cable cores.^{7,31} Our paper reported the interesting effect of frequencies on the superconducting losses and eddy current losses in the substrate and stabilizers for the CORC configuration.

G. Effect of number of gaps on ac loss in cables

Coated conductors are now commercially available in several widths. When narrower tapes are used to make a cable, the number

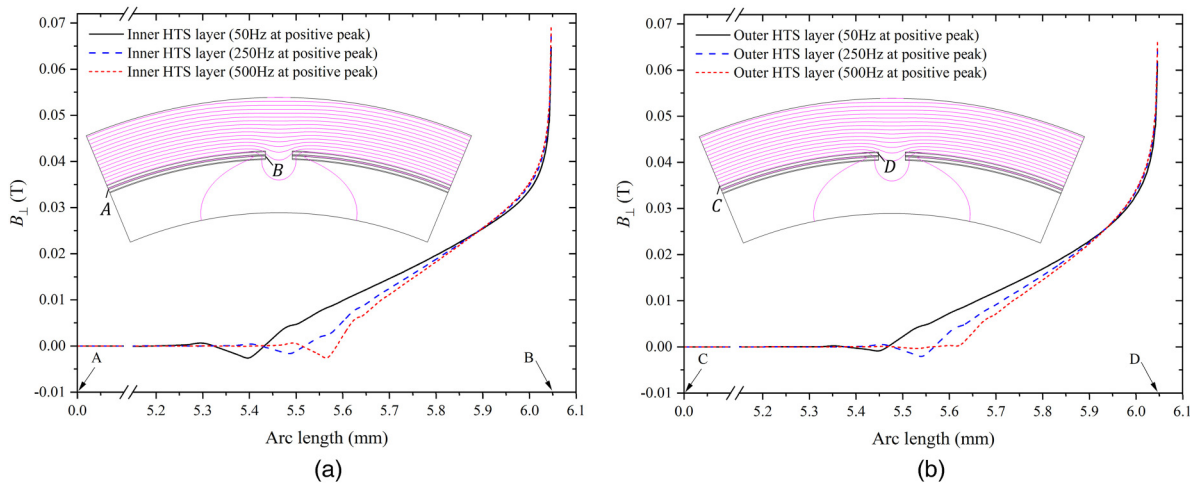


FIG. 16. Perpendicular magnetic flux density (B_{\perp}) distribution along the half-width of HTS tapes in (a) the inner and (b) outer HTS layers of a fully aligned cable ($\beta = 0^\circ$). The cable carries a transport current $I/I_c = 0.7$ at various current frequencies: 50, 250, and 500 Hz.

30 October 2023 13:53:15

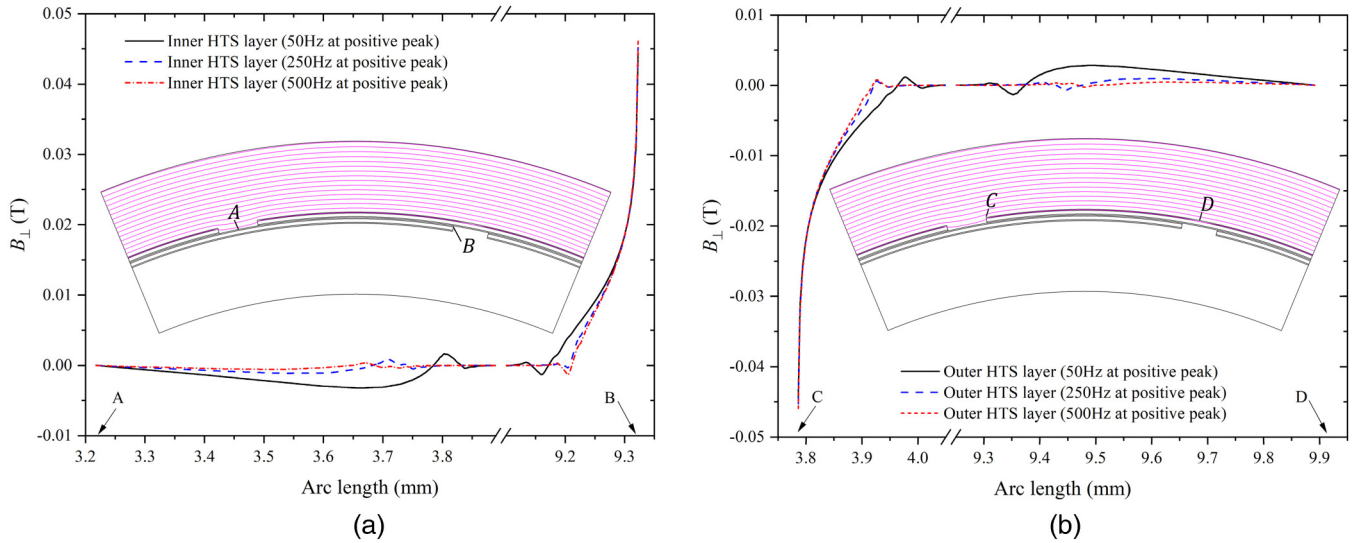


FIG. 17. Perpendicular magnetic flux density (B_{\perp}) distribution along the half-width of HTS tapes in (a) the inner and (b) outer HTS layers of a fully misaligned cable ($\beta = 22.5^{\circ}$). The cable carries a transport current $I/I_c = 0.7$ at various current frequencies: 50, 250, and 500 Hz.

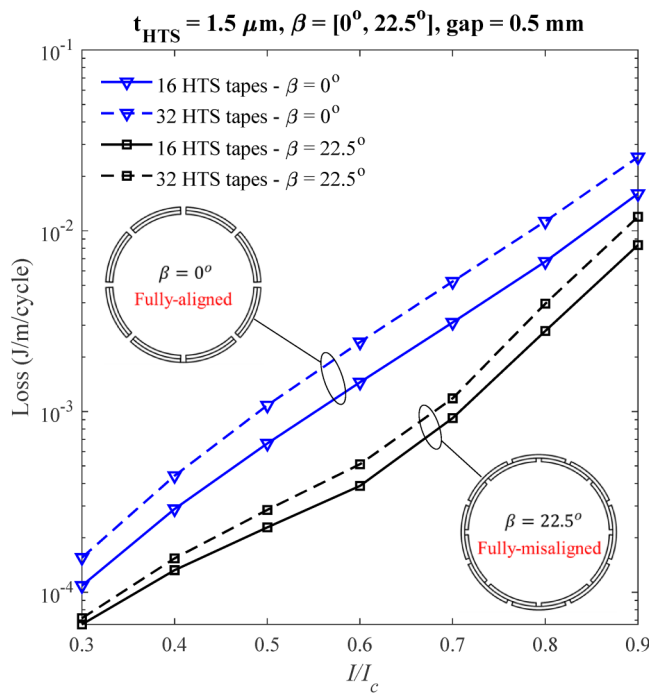


FIG. 18. Transport ac losses in cables 1 and 2 for $\beta = 0^{\circ}$ and $\beta = 22.5^{\circ}$. Both cables have the same diameter, l_c and gap size, but one fabricated by 16 tapes of 12.5 mm width and the other fabricated by 32 tapes of 5.75 mm width.

of tapes (and therefore the number of gaps) must be increased to achieve the same cable I_c . This section compares ac losses in two two-layer cables of the same diameter, I_c , and gap size, the first fabricated from 16 tapes of 12.5 mm width and the other fabricated from 32 tapes of 5.75 mm width. Detailed specifications can be found in Table I. The cables have the same winding diameter, so their circumferential fields should have the same amplitude if the cables carry the same transport current. Figure 18 plots transport ac losses in cables 1 and 2 for both cases, $\beta = 0^{\circ}$ and $\beta = 22.5^{\circ}$. The ac losses in cable 2 are higher than those generated in cable 1, especially in the case of $\beta = 0^{\circ}$ when the edge loss is dominant. For this case, ac loss in cable 2 is about 60% higher for nearly the entire current range.

IV. CONCLUDING REMARKS AND DISCUSSIONS

We have provided insights into the behavior of the ac losses of CORC HTS cables by utilizing both 1D and 2D models. Our results can be summarized as follows:

- (1) The ac losses are highest when $\beta = 0^{\circ}$ (the gaps of the inner and outer layers are perfectly aligned). The ac losses decrease and flatten when gaps are not aligned ($5^{\circ} < \beta < 22.5^{\circ}$). Because the latter represents a greater angular range, the losses calculated for misaligned gaps represent better the ac losses in the cables.
- (2) Ac losses in HTS cable are the result of two components: the surface loss generated by parallel circumferential field and edge loss generated by the perpendicular fields generated locally near the gaps. For configurations with misaligned gaps, the

30 October 2023 13:53:15

surface loss is dominant for the low current region $I/I_c < 0.5$. However, the edge loss increases quickly with increasing current and becomes a dominant contribution at $I/I_c > 0.6$.

- (3) Because the edge loss, which strongly depends on the gap size, becomes the dominant contribution for high transport currents, reducing the number of gaps by using wider HTS tape should reduce ac losses significantly. However, it is challenging to conform a wider HTS tape to a small former. Flexible, wide HTS tapes with thin substrates would be beneficial for cables with lower ac losses.
- (4) Gap size should be minimized to reduce ac losses. Besides the low ac loss target, cables are also designed to have a balanced current-sharing operation with the lowest cable inductance (or axial magnetic field). These objectives—the smallest gaps, balanced current sharing, and low cable inductance—are difficult to achieve simultaneously, but the availability of HTS tapes at a larger variety of widths should ease the process.
- (5) In the operating current region ($I/I_c > 0.5$) and frequencies below 500 Hz, ac losses generated in the HTS layer are still dominant. HTS losses (per cycle) decrease as the frequency increases; the perpendicular magnetic fields near gaps decrease when the frequency increases. The shielding effects of the HTS layers and metal layers might produce this effect.

ACKNOWLEDGMENTS

This work was supported in part by the ARPA-E of DoE under Contract No. DE-FOA-0002459 and in part by NSF under Grant Nos. DMR-1644779 and DMR-2128556.

AUTHOR DECLARATIONS

Conflict of Interest

The authors have no conflicts to disclose.

Author Contributions

Linh N. Nguyen: Software (equal); Validation (equal); Visualization (equal); Writing – original draft (equal); Writing – review & editing (equal). **Nathaniel Shields:** Software (equal); Visualization (equal); Writing – original draft (equal). **Stephen Ashworth:** Funding acquisition (equal); Methodology (equal); Project administration (equal). **Doan N. Nguyen:** Conceptualization (equal); Methodology (equal); Software (equal); Supervision (equal); Writing – original draft (equal); Writing – review & editing (equal).

DATA AVAILABILITY

The data that support the findings of this study are available from the corresponding author upon reasonable request.

REFERENCES

¹J. D. Weiss, T. Mulder, H. J. ten Kate, and D. C. van der Laan, “Introduction of CORC® wires: Highly flexible, round high-temperature superconducting wires for magnet and power transmission applications,” *Supercond. Sci. Technol.* **30**, 014002 (2017).

- ²W. Yuan, S. Venuturumilli, Z. Zhang, Y. Mavrocostanti, and M. Zhang, “Economic feasibility study of using high-temperature superconducting cables in UK’s electrical distribution networks,” *IEEE Trans. Appl. Supercond.* **28**, 1–5 (2018).
- ³S. J. Lee, M. Park, I.-K. Yu, Y. Won, Y. Kwak, and C. Lee, “Recent status and progress on HTS cables for AC and DC power transmission in Korea,” *IEEE Trans. Appl. Supercond.* **28**, 1–5 (2018).
- ⁴C. Lee, H. Son, Y. Won, Y. Kim, C. Ryu, M. Park, and M. Iwakuma, “Progress of the first commercial project of high-temperature superconducting cables by KEPCO in Korea,” *Supercond. Sci. Technol.* **33**, 044006 (2020).
- ⁵L. N. Nguyen, M. Naud, J. Weiss, S. Pamidi, S. A. Dönges, D. van der Laan, and D. N. Nguyen, “Simulation for the fault current limiting operation of REBCO CORC® superconducting cables with different core materials,” *IEEE Trans. Appl. Supercond.* **33**, 1–8 (2022).
- ⁶M. Sumption, J. Murphy, T. Haugan, M. Majoros, D. van der Laan, N. Long, and E. Collings, “AC losses of Roebel and CORC® cables at higher AC magnetic fields and ramp rates,” *Supercond. Sci. Technol.* **35**, 025006 (2022).
- ⁷R. Terzioglu, M. Vojenciak, J. Sheng, F. Gömöry, T. F. Çavuş, and İ. Belenli, “AC loss characteristics of CORC® cable with a Cu former,” *Supercond. Sci. Technol.* **30**, 085012 (2017).
- ⁸J. Ogawa, S. Fukui, N. Koseki, T. Fujii, and Y. Mihira, “Experimental investigation of AC loss characteristics under HTS cable electromagnetic conditions,” *IEEE Trans. Appl. Supercond.* **30**, 1–5 (2020).
- ⁹T. Yamaguchi, Y. Shingai, M. Konishi, M. Ohya, Y. Ashibe, and H. Yumura, “Large current and low AC loss high temperature superconducting power cable using REBCO wires,” *SEI Tech. Rev.* **78**, 79 (2014); available at <https://global-sei.com/technology/tr/bn78/pdf/78-16.pdf>
- ¹⁰S. Ashworth and D. Nguyen, “The electrical measurement of AC losses in a three-phase tri-axial superconducting cable,” *Supercond. Sci. Technol.* **23**, 095009 (2010).
- ¹¹J. Han, W.-S. Kim, K. Choi, and J.-K. Lee, “Magnetization loss of multi-layered CORC according to various winding types,” *IEEE Trans. Appl. Supercond.* **32**, 1–5 (2022).
- ¹²D. A. Nguyen, S. P. Ashworth, R. Duckworth, W. Carter, and S. Fleshler, “Measurements of AC losses and current distribution in superconducting cables,” *IEEE Trans. Appl. Supercond.* **21**, 996–1000 (2010).
- ¹³K. Yagotintsev, V. Anvar, P. Gao, M. Dhalle, T. Haugan, D. Van Der Laan, J. Weiss, M. Hossain, and A. Nijhuis, “AC loss and contact resistance in REBCO CORC®, Roebel, and stacked tape cables,” *Supercond. Sci. Technol.* **33**, 085009 (2020).
- ¹⁴A. P. Malozemoff, G. Snitchler, and Y. Mawatari, “Tape-width dependence of AC losses in HTS cables,” *IEEE Trans. Appl. Supercond.* **19**, 3115–3118 (2009).
- ¹⁵F. Grilli, E. Pardo, A. Stenvall, D. N. Nguyen, W. Yuan, and F. Gömöry, “Computation of losses in HTS under the action of varying magnetic fields and currents,” *IEEE Trans. Appl. Supercond.* **24**, 78–110 (2013).
- ¹⁶M. Siahraug, F. Sirois, D. N. Nguyen, and S. P. Ashworth, “Assessment of alternative design schemes to reduce the edge losses in HTS power transmission cables made of coated conductors,” *Supercond. Sci. Technol.* **25**, 014001 (2012).
- ¹⁷F. Grilli, F. Sirois, S. Brault, R. Brambilla, L. Martini, D. N. Nguyen, and W. Goldacker, “Edge and top/bottom losses in non-inductive coated conductor coils with small separation between tapes,” *Supercond. Sci. Technol.* **23**, 034017 (2010).
- ¹⁸V. M. Zermeno, F. Grilli, and F. Sirois, “A full 3D time-dependent electromagnetic model for Roebel cables,” *Supercond. Sci. Technol.* **26**, 052001 (2013).
- ¹⁹B. Shen, F. Grilli, and T. Coombs, “Review of the AC loss computation for HTS using H formulation,” *Supercond. Sci. Technol.* **33**, 033002 (2020).
- ²⁰B. Shen, X. Chen, L. Fu, S. Jiang, H. Gou, J. Sheng, Z. Huang, W. Wang, Y. Zhai, Y. Yuan *et al.*, “Superconducting conductor on round core (CORC) cables: 2D or 3D modeling?,” *IEEE Trans. Appl. Supercond.* **31**, 1–5 (2021).
- ²¹S. Fu, M. Qiu, J. Zhu, H. Zhang, J. Gong, X. Zhao, W. Yuan, and J. Guo, “Numerical study on AC loss properties of HTS cable consisting of YBCO coated conductor for HTS power devices,” *IEEE Trans. Appl. Supercond.* **28**, 1–5 (2018).

- ²²M. Siahraang, F. Sirois, D. N. Nguyen, S. Babic, and S. P. Ashworth, “Fast numerical computation of current distribution and AC losses in helically wound thin tape conductors: Single-layer coaxial arrangement,” *IEEE Trans. Appl. Supercond.* **20**, 2381–2389 (2010).
- ²³F. Huber, W. Song, M. Zhang, and F. Grilli, “The TA formulation: An efficient approach to model the macroscopic electromagnetic behaviour of HTS coated conductor applications,” *Supercond. Sci. Technol.* **35**, 043003 (2022).
- ²⁴Y. Wang, Y. Wang, D. Wei, T. Guo, Y. Meng, J. Wang, and C. Kan, “AC losses of a like-CORC conductor using accelerated 3D TA model,” *Physica C* **579**, 1353770 (2020).
- ²⁵J. Yang, M. Tian, J. Ma, Y. Ozturk, C. Li, J. Hu, J. Gawith, A. Shah, I. Patel, H. Wei *et al.*, “Numerical study on AC loss characteristics of conductor on round core cables under transport current and magnetic field,” *IEEE Trans. Appl. Supercond.* **31**, 1–4 (2021).
- ²⁶S. Wang, H. Yong, and Y. Zhou, “Calculations of the AC losses in superconducting cables and coils: Neumann boundary conditions of the T–A formulation,” *Supercond. Sci. Technol.* **35**, 065013 (2022).
- ²⁷Q. Li, Y. Lu, W. Zhao, D. Zhou, and C. Cai, “Effects of winding angle on losses of CORC cable—A numerical study,” *IEEE Trans. Appl. Supercond.* **33**, 1–7 (2022).
- ²⁸B. Shen, X. Chen, L. Fu, M. Zhang, Y. Chen, J. Sheng, Z. Huang, W. Wang, Y. Zhai, Y. Yuan *et al.*, “A simplified model of the field dependence for HTS conductor on round core (CORC) cables,” *IEEE Trans. Appl. Supercond.* **31**, 1–5 (2021).
- ²⁹S. Sato and N. Amemiya, “Electromagnetic field analysis of YBCO coated conductors in multi-layer HTS cables,” *IEEE Trans. Appl. Supercond.* **16**, 127–130 (2006).
- ³⁰Q. Li, N. Amemiya, R. Nishino, T. Nakamura, and T. Okuma, “AC loss reduction of outer-diameter-fixed superconducting power transmission cables using narrow coated conductors,” *Physica C* **484**, 217–222 (2013).
- ³¹J. Yang, C. Li, M. Tian, S. Liu, B. Shen, L. Hao, Y. Ozturk, and T. Coombs, “Analysis of AC transport loss in conductor on round core cables,” *J. Supercond. Novel Magn.* **35**, 57–63 (2022).
- ³²N. Amemiya, Z. Jiang, M. Nakahata, M. Yagi, S. Mukoyama, N. Kashima, S. Nagaya, and Y. Shiohara, “AC loss reduction of superconducting power transmission cables composed of coated conductors,” *IEEE Trans. Appl. Supercond.* **17**, 1712–1717 (2007).
- ³³J. Ogawa, S. Fukui, T. Oka, T. Ogawa, and M. Sugai, “AC loss distribution in two-layer HTS cable,” *IEEE Trans. Appl. Supercond.* **28**, 1–4 (2017).
- ³⁴J. Ogawa, S. Fukui, T. Oka, T. Sato, A. Tamura, E. Kasuga, and K.-W. Ryu, “Influence of AC transport current balance on AC loss in a two layered polygonal YBCO assembled conductor,” *IEEE Trans. Appl. Supercond.* **22**, 4704804 (2011).
- ³⁵See www.advancedconductor.com for information about CORC cable.
- ³⁶See www.comsol.com for information about FEM COMSOL Multiphysics.
- ³⁷F. Grilli, F. Sirois, V. M. Zermeno, and M. Vojenciak, “Self-consistent modeling of the I_c of HTS devices: How accurate do models really need to be?,” *IEEE Trans. Appl. Supercond.* **24**, 1–8 (2014).
- ³⁸J. Xia, H. Bai, J. Lu, A. V. Gavrilin, Y. Zhou, and H. W. Weijers, “Electromagnetic modeling of REBCO high field coils by the H-formulation,” *Supercond. Sci. Technol.* **28**, 125004 (2015).